CHAPTER IV
ADSORPTION OF TOXIC GASES FROM GASIFICATION PROCESS BY POLY(HIPEs)

4.1 Abstract

Poly(DVB)HIPEs prepared with a porogenic solvent (toluene) and two types of mixed surfactants (SPAN80, DDBSS, and CTAB; 6.3, 0.4, and 0.3 wt% (S80DCI) and 9.5, 0.3, and 0.2 wt% (S80DCII)). The obtained poly(DVB)HIPEs exhibited surface areas up to 550 m^2/g. However, due to their poor mechanical properties, 1, 3, 5, 10 and 15 wt% of acid-treated clay were added into the monomer phase of poly(DVB)HIPE to improve the mechanical properties and increase the adsorptive capacity of resulting materials. The resulting materials were characterized by SEM, N_2 adsorption-desorption, TG/DTA, and compression test.

Surface areas of S80DCI decreased from 550 to 251 m^2/g. The compressive modulus of the obtained poly(DVB)HIPEs increased from 2.59 to 3.50 MPa with 0 to 5 wt% acid-treated clay content, and decreased to 2.07 MPa when the acid-treated clay content was 15 wt%.

Surface areas of S80DCII with 0 to 10 wt% of added acid-treated clay increased from 198 to 523 m^2/g, and the compressive modulus increased from 2.61 to 3.00 MPa with 0 to 5 wt% acid-treated clay content. The surface area and compressive modulus were decreased to 346 m^2/g and 1.99 MPa, respectively, when the amount of added acid-treated clay content was 15 wt%.

CO_2 adsorption tests were carried out on the obtained poly(DVB)HIPE and it was found that CO_2 adsorption was between 2.43 to 18.2 mmol/g. The highest adsorption was obtained from S80DCI with 1 wt% acid-treated clay.

Keywords: Poly(DVB)HIPEs, Mixed surfactants, Acid-treated clay, Poly(DVB)HIPE nanocomposites, CO_2 gas adsorption

4.2 Introduction

One of the most commonly found problems in the atmosphere is high levels of gas-like pollutants; coming from different sources, mainly released by industrial activities and gasification processes. Therefore, it is very important to design adsorbent materials that would adsorb such gases before being liberated into the environment.

High internal-phase emulsion (HIPEs) polymerization process for manufacture microcellular, was patented by Unilever [1]. This patent discloses a polymerization process that occurs in a water-in-oil emulsions in which the dispersed phase, occupies more than 74% of the volume, containing high volume fraction of water, a water-soluble initiator (potassium persulfate) and stabilizer (calcium chloride) [2]. The continuous organic phase, which generally constitutes less than 26% of the final volume, can contain monomers (styrene), crosslinking comonomers (divinyl benzene) and organic soluble surfactant (sorbitan monooleate, SPAN80) [3]. A polyHIPE is a microporous material produced by the polymerization of the monomers in the continuous phase of a HIPE. Subsequent removal of the aqueous produces a highly porous material (porosities of up to 97%). In addition, feature of the morphology such as cell size, interconnecting hole size and porosity can be efficiently controlled.

Another structural feature that is useful and able to be controlled is the surface area. PolyHIPEs have relatively low surface areas (3-20 m^2/g are typical) which hampers their applicability in area such as chromatography, solid-phase extraction, adsorption and filtration. However, much higher values can be obtained by replacement of some of the monomeric continuous phase with inert diluents (porogen) [4]. During polymerization, phase separation occurs within the developing polymer structure between the internal phase droplets. This leads to materials with dual porosity: very large macropores typical of PolyHIPEs, with pore diameters upward of 1 μm, and much smaller pores within the PolyHIPE walls, lead to higher surface area. These latter pores are typical of those found in permanently porous resin beads, and indeed the pore size distribution obtained (micro-, meso- or macropores) depends on the nature of porogen and amount of cross-linker used.

The effectiveness of a mixture of nonionic, anionic, and cationic surfactants: sorbitan monolaureate (SPAN20), dodecylbenzenesulfonic acid sodium salt (DDBSS), and cetyltrimethylammonium bromide (CTAB) with an amphiphilic compound for emulsion stabilization has been known for a long time [5]. Mixtures of ionic and non-ionic surfactants are known to form a more robust interfacial film around each emulsion droplet, leading to enhance emulsion stability when a mixture of emulsifiers (SPAN20, CTAB and DDBSS) and toluene as a porogen were used, polyHIPE samples were found to be porous and open-cell microstructures with the surface area of 370-430 $m^2 g^{-1}$.

However, the main problem of cellular materials with high surface areas is their poor mechanical properties, which limit their practical uses in industrial. Many of industrial uses of clays minerals are related to their adsorptive capacity, which increases with acid treatment. Acid treatment of clay minerals (by using mainly HCl or H_2SO_4 solutions) [6] is chemical treatment of the clays to modify structural, textural and/or acidic properties, which influence the adsorption capacity. By incorporating the acid-treated clay into the monomer phase of the high internal phase emulsion, it would not only improve the adsorptive capacity but also would increase the mechanical properties of the resulting materials when compared to the unfilled materials [7].

The purpose of this work is to prepare poly(DVB)HIPE filled with acid-treated clay and determine the suitable amounts of added clay for adsorption of toxic gases from gasification process.

4.3 Experimental

4.3.1 Materials

Divinylbenzene (DVB) was supplied by Merck. Toluene (T) and Hydrochloric acid (HCl) were supplied by Lab Scan. Ethanol (EtOH) was supplied by Carlo Erba. Isopropanol was supplied by Etalma. Sorbitan monooleate (SPAN80) and Dodecylbenzenesulfonic acid, sodium salt (DDBSS) were supplied by Sigma. Cetyltrimethyl- ammonium [$C_{16}H_{31}N^+(CH_3)_3$] bromide (CTAB) and 2,5-dimethoxy-4-(n)-amylamphetamine (DOAM) were supplied by Fluka. Bentonite (BTN) was

supplied by Thai Nippon Chemical Industry Co., Ltd. The cation exchange capacity (CEC) of BTN is 43 mmol/100g of clay. Potassium persulfate ($K_2S_2O_8$) and Calcium chloride dehydrate ($CaCl_2 \cdot 2H_2O$) were supplied by Fluka.

4.3.2 Methods

4.3.2.1 Preparation of Acid-treated Clay

Na-bentonite clay was slowly added to 3N HCl solutions, stirred and maintained at 110°C for 3 h. The clay/acid ratio used in the study was 2% wt/wt. After treatment, the clay was separated and washed with distilled water several times and dry until constant weight was obtained and grind. 1 g of the obtained acid-treated clay was added to 30 mL of distilled water and stirred at 80°C for 24 h. 3.78 g of DOAM, 15 mL of EtOH, and 15 mL of H_2O were added to acid-treated clay solution for modified clay. Then stirred solution for 3 h until transparent, added warm water and filtered, and washed by soxhlet overnight with ethanol [8].

4.3.2.2 Preparation of Poly(DVB)HIPE filled with Acid-treated Clay

The cellular materials were prepared by first dissolving organic phase containing 5 mL of DVB monomer, 5 mL of toluene, required amounts of acid-treated clay, and a mixture of nonionic, anionic, and cationic surfactants: SPAN80, DDBSS, and CTAB was added to the mixture, stirred for 10 min. While 90 mL of distilled water containing 0.2 g of potassium persulfate and 1 g of calcium chloride dihydrate were added dropwise. After all the water has been added, the emulsion was further stirred for 20 min and placed in a glass bottle. The obtained emulsions were capped and put in a convection oven at 70°C for 48 h to polymerize [5]. After polymerization, the cellular materials were removed from the glass bottles and washed by soxhlet for 6 h with 2-propanol [7]. Then the cellular materials were returned to vacuum oven to dry at 80°C for 48 h.

4.3.3 Equipment

4.3.3.1 X-ray Diffractometer (XRD)

X-ray diffractometer (XRD) was used to observe the d-value of BTN, organo BTN, and organo acid-treated BTN and to investigate the crystal structure of nanocomposites. X-ray diffraction patterns were measured on a Rigaku

Model Dmax 2002 diffractometer with Ni-filtered Cu Kα radiation operated at 40 kV and 30 mA. The powder samples were observed on the 2θ range of 1.8-20 degree with scan speed 2 degree/min and scan step of 0.02 degree.

4.3.3.2 Surface Area Analyzer (AS-1)

N_2 adsorption-desorption isotherms were obtained at -196°C on a Quantachrome Autosorb-1. Samples were degassed at 100°C during 12 h in a vacuum furnace prior to analysis. Surface areas were calculated using the BET equation. The pore size distributions were constructed based on Barrett, Joyner and Halenda (BJH) method using the adsorption branch of the nitrogen isotherm.

4.3.3.3 Fourier Transform Infrared Spectroscopy (FT-IR)

The FT-IR spectra of BTN, organo BTN and organo acid-treated BTN were obtained using a Nicolet Nexus 670 FT-IR spectrometer in the frequency range of 4000-400 cm^{-1} with 32 scans at a resolution of 2 cm^{-1}. KBr pellet technique was applied in the preparation of powder samples. The incorporation of organic group into silicate network is investigated by using FTIR.

4.3.3.4 Thermogravimetric Analysis (TGA)

Thermo-gravimetric analysis (TGA) was performed to measure the thermal stability of the poly(DVB)HIPEs. TGA of both neat and poly(DVB)HIPE nanocomposites were performed using a Mettler Toledo TGA/SDTA 851e instrument. Experiments were carried out under nitrogen gas atmosphere. Samples were cut into small pieces weigh about 2–5 mg. Then the samples were loaded on the platinum pan and heated to 600°C from 40°C at a heating rate of 10°C/min. One steps degradation was observed during testing, and the decomposition temperature was recorded corresponding to 50% decomposition of the material.

4.3.3.5 Differential Scanning Calorimetry (DSC)

The glass transition temperature of poly(DVB)HIPEs was determined using a Perkin-Elmer DSC 7 instrument. The sample was first heated from 30°C to 250°C and cooled down at a rate of 10°C/min under a N_2 atmosphere with a flow rate of 10 ml/min. The sample was then reheated to 250°C at the same rate.

4.3.3.6 Scanning Electron Microscope (SEM)

Scanning electron microscopy was performed on JEOL/JSM 5200 Model to observe surface morphology of poly(DVB)HIPEs. The specimens were coated with gold under vacuum before observation to make them electrically conductive.

4.3.3.7 X-ray Fluorescence (XRF)

Chemical compositions of BTN, organo BTN before and after treated with 3N HCl solutions were obtained using Oxford Model ED2000 X-ray tube with silver as a filter, operate at voltage 35 kV.

4.3.3.8 Transmission Electron Microscope (TEM)

Transmission electron microscopy was also used in this studied to observe the morphology of the poly(DVB)HIPE nanocomposites. TEM micrographs were taken on a Tecnai G2 Sphera electron microscope with an accelerating voltage of 80 kV to observe the pore structure and secondary pore in the cell wall of poly(DVB)HIPEs. Micrographs were recorded at magnifications of 80000× and 150000× magnification. TEM samples were prepared by embedding poly(DVB)HIPE nanocomposites in a support resin and sectioning on an ultra-thin microtome. The thin sections were supported on 300 mesh copper grids.

4.3.3.9 Universal Testing Machine (LLOYD)

A Lloyds Universal Testing Machine (Lloyds/LRX) equipped with a 500 N load cell was used to measure mechanical properties in compression. The samples were loaded at a rate of 1.27 mm/min. Samples of 25.4 mm in diameter and 25.4 mm in height were used for tested of each poly(DVB)HIPEs. The samples were loaded until a displacement of 70 percent of the height of the examined sample was reached.

4.3.3.10 CO_2 Gas Adsorption

Study of CO_2 gas adsorption capacities of poly(DVB)HIPE filled with acid-treated clay were carried out using a pilot gasification unit at the faculty of chemical technology Chulalongkorn university. Samples were cut into small pieces weigh about 1–2 g. Then the samples were loaded into sample tube 2×25 cm. CO_2 3 mL/min and He 17 mL/min were flowed through the sample at room

temperature. The residue of CO_2 was measured by a Gas Chromatography instument, column used Shimadzu 2014, flow rate 35 mL/min.

4.4 Results and Discussion

4.4.1 Characterization of acid-treated clay and organo acid-treated clay

4.4.1.1 Surface areas of acid-treated clay

The surface area of acid-treated clay was characterized using BET. Table 4.1 shows surface area of BTN before and after treated with 1.5N, 1.7N, and 3.0N HCl solutions. The surface area of BTN was found to increase with increasing concentration of HCl solutions up to 3.0N HCl. Therefore, 3N HCl solution was the most suitable concentration for treating clay minerals in order to obtain high surface area. This is consistant with results observed by Venaruzzo *et al* [8].

Table 4.1 Surface areas of BTN before and after treated with HCl solutions

Sample	Surface area (m^2/g)
BTN	13.28
BTN treated with 1.5N HCl	29.38
BTN treated with 1.7N HCl	34.76
BTN treated with 3.0N HCl	62.36

4.4.1.2 Modification of acid-treated bentonite and chemical compositions

Clay is hydrophilic in nature and will separate from organic phase of HIPE. Therefore, modification of clay is necessary to increase its hydrophobicity, so that it will not separate from the organic phase of HIPE. This research used DOAM of 1.5 CEC as a surfactant for modifying the acid-treated BTN. The structural characteristics of BTN, organo BTN and organo acid-treated BTN were characterized using FTIR, XRD, and XRF. An important structural change of clay was observed before and after acid treatment.

The presence of surfactant in the clay was evidenced by FTIR spectrum of BTN, which is shown in Figure 4.1(a). FTIR spectra of organo BTN and

organo acid-treated BTN (Figure 4.1(b-c)) shows stretching vibration of the unsaturated ketones, and the asymmetric and symmetric stretching vibrations of alkanes around 1700, and 2900 cm^{-1}, respectively which are characteristics peaks of the surfactant templates.

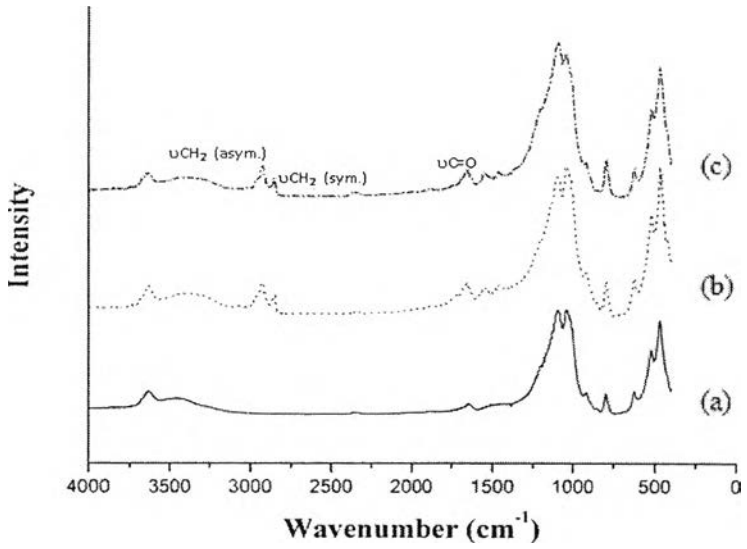

Figure 4.1 FTIR spectra of (a) BTN, (b) organo BTN, and (c) organo acid-treated BTN.

Table 4.2 Chemical compositions of BTN, 3N HCl treated BTN, organo BTN, and 3N HCl treated organo BTN. (oct: cations in octahedral position: Al, Mg, Fe and Ti)

Sample	SiO_2 %	Al_2O_3 %	MgO %	Fe_2O_3 %	TiO_2 %	Si/oct molar
BTN	77.776	9.938	1.023	2.197	0.367	4.957
3N HCl treated BTN	87.962	5.639	0.421	0.985	0.400	10.063
Organo BTN	80.505	10.266	1.043	2.301	0.391	4.955
3N HCl treated organo BTN	87.972	7.172	0.515	1.206	0.432	8.639

Table 4.2 shows chemical compositions of BTN, 3N HCl treated BTN, organo BTN, and 3N HCl treated organo BTN. The Si/(Al+Mg+Fe+Ti) molar ratios of the BTN and organo BTN were increased after acid treatment. The acid

treatment of clay removed an important amount of octahedral cations in the following order: Al>Fe>Mg>Ti. The clay structure decomposition resulted in increasing specific surface area of BTN from 13.28 m^2/g to 62.36 m^2/g.

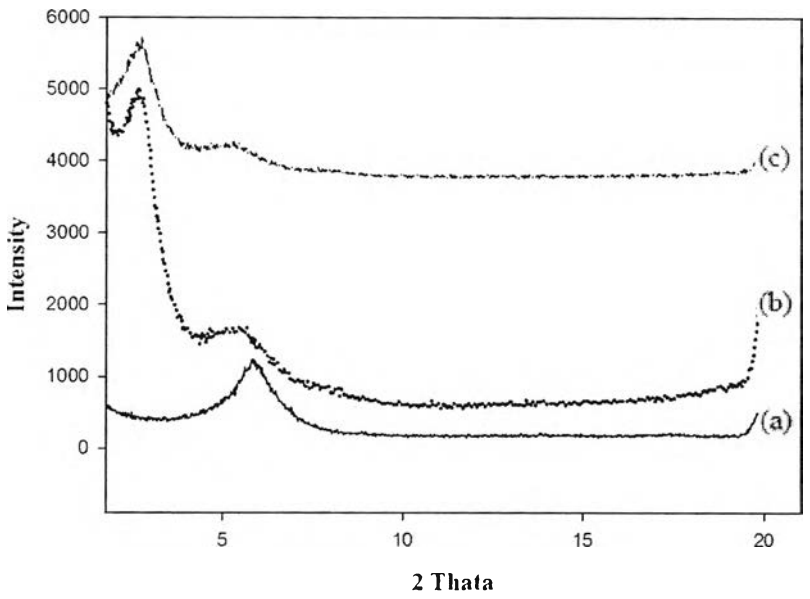

Figure 4.2 XRD pattern of (a) BTN, (b) organo BTN, and (c) organo acid-treated BTN.

A corresponding XRD patterns (Figure 4.2(a), (b), and (c)) show the presence of the (001) reflection peak which is the basal spacing of clay. From Figure 4.2(a), the basal spacing of BTN was 1.544 nm. For organo BTN (Figure 4.2(b)), the d_{001} peak was observed at a lower angle than that of BTN and the basal spacing was 4.042 nm. After acid treatment (Figure 4.2(c)), d_{001} peak was observed at a lower angle than that of BTN and the basal spacing was 3.906 nm with decreased in peak intensity, The intensity of (001) reflection was reduced and more amorphized materials was observed with the increase of the acid concentration[9]. Therefore, from FTIR spectra and XRD pattern, its were confirmed that successful modification of acid-treated BTN was achieved.

4.4.2 Characterization of poly(DVB)HIPEs filled with acid-treated clay

4.4.2.1 Morphologies and surface areas

SEM micrographs (Figure 4.3) show morphological characteristics of poly(DVB)HIPEs, prepared using a surfactant mixture of 6.3 wt% of SPAN80, 0.4 wt% of DDBSS, and 0.3 wt% of CTAB (S80DCI) filled with different acid-treated clay content.

The void sizes and interconnecting window sizes of the obtained materials were found to increase with increasing content of acid-treated clay added. These results could be due to the increasing of acid-treated clay content results in the system of poly(DVB)HIPE becoming unstable, leading to more brittle and thus resulting in lower surface area (listed in Table 4.3) and decrease volume adsorbed (See Figure 4.4).

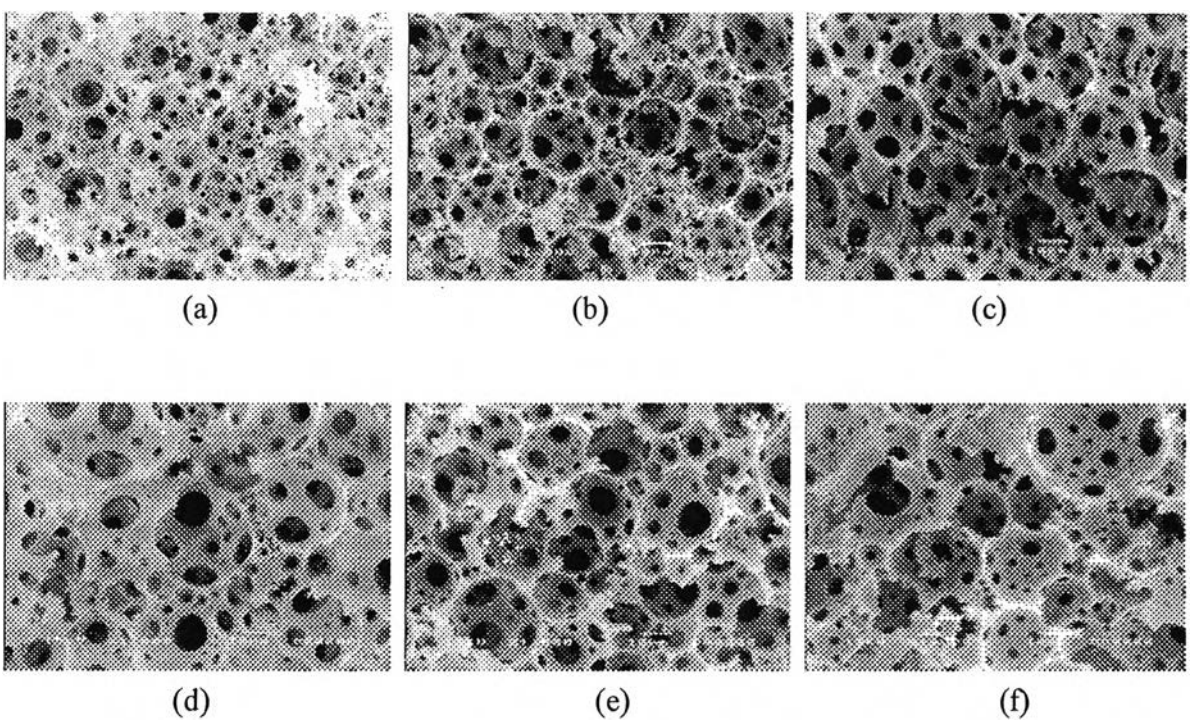

Figure 4.3 SEM micrographs of S80DCI filled with different acid-treated clay content (wt%); (a) 0; (b) 1; (c) 3; (d) 5; (e) 10; and (f) 15.

Table 4.3 Surface areas, cumulative pore volumes, and average pore diameters of S80DCl filled with different amount of acid-treated clay content (wt%)

Sample	Surface areas (m^2/g)[a]	Cumulative pore volumes (cm^3/g)[b]	Average pore diameters (nm)[b]
0 wt%	550 ± 11	0.27 ± 0.006	1.35 ± 0.006
1 wt%	501 ± 10	0.24 ± 0.007	1.49 ± 0.007
3 wt%	372 ± 27	0.19 ± 0.003	1.36 ± 0.002
5 wt%	353 ± 4	0.18 ± 0.001	1.36 ± 0.001
10 wt%	346 ± 20	0.18 ± 0.008	1.36 ± 0.003
15 wt%	251 ± 7	0.13 ± 0.012	1.37 ± 0.005

[a] From BET treatment of N_2 adsorption data.

[b] From BJH treatment of N_2 adsorption data.

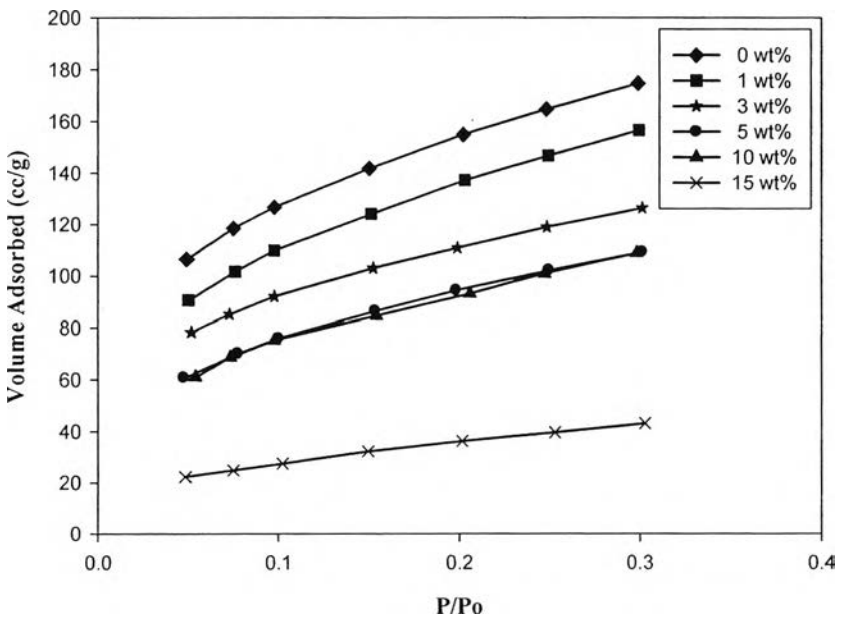

Figure 4.4 Volume adsorbed for S80DCI filled with different acid-treated clay content (wt%).

In 1986, Scamehorn studied the effect of added nonionic surfactant on precipitation of anionic-cationic surfactant mixtures at equilibrium, and suggested that nonionic surfactants can enhance micelle formation with either anionic surfactants or with cationic surfactants. Therefore, it was possible that nonionic surfactants could also enhance the formation of micelles in mixed anionic-cationic systems. As the concentration of added nonionic surfactant increases, the tendency for precipitate is reduced, except at high concentrations of anionic or cationic surfactants [10]. Therefore, it was possible to change the surfactant mixture ratios to increase the emulsion stability of poly(DVB)HIPE system by increasing ratio of nonionic surfactant (SPAN 80), and decreasing ratios of anionic and cationic surfactants (DDBSS and CTAB).

The changes in different surfactant mixture ratios (prepared using a surfactant mixture of 9.5 wt% of SPAN80, 0.3 wt% of DDBSS, and 0.2 wt% of CTAB) (S80DCII), and different acid-treated clay content can be explained using SEM micrographs of the obtained poly(DVB)HIPEs (see Figure 4.5).

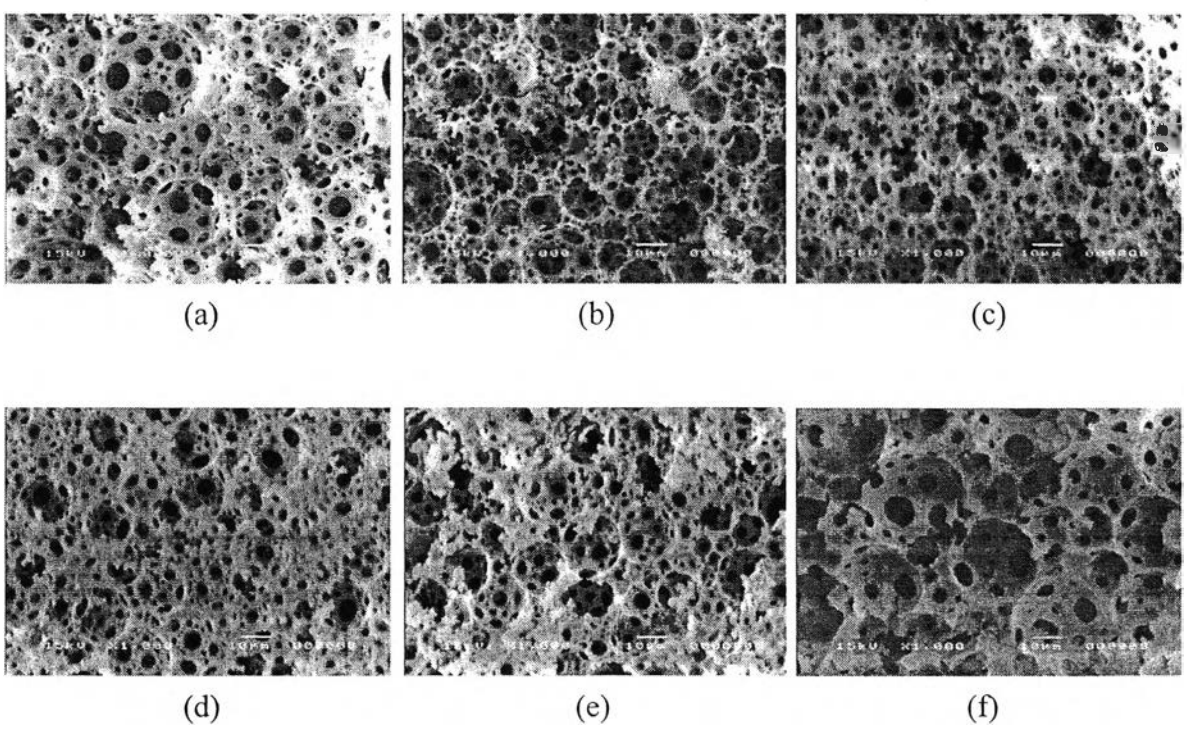

Figure 4.5 SEM micrographs of S80DCII filled with different acid-treated clay content (wt%); (a) 0; (b) 1; (c) 3; (d) 5; (e) 10; and (f) 15.

PolyHIPEs prepared using a surfactant mixture of 9.5 wt% of SPAN80, 0.3 wt% of DDBSS, and 0.2 wt% of CTAB (S80DCII). The void sizes and interconnecting window sizes were found to decrease with increasing content of acid-treated clay added. These results could be due to the increasing of acid-treated clay content which resulted in the system of poly(DVB)HIPE becoming more stable. The acid treatment of clay minerals removed the octahedral layer cations of bentonite clay, resulting in increasing in porosity and acidicity of bentonite clay, leading to higher surface area (listed in Table 4.4). It was evident from the volume adsorbed of poly(DVB)HIPE (See Figure 4.6) that adsorption was increased when the acid-treated clay were added [11]. This in turn an increase in BET surface area and volume adsorbed of poly(DVB)HIPEs after acid treatment influenced to get a larger adsorption of CO_2 gas [8].

At 15 wt% of acid-treated clay content, surface area decreased. This was propably due to emulsion becoming unstable and the void size of poly(DVB)HIPE increased (See Figure 4.5) also the amount of the added acid-treated clay was high, resulted in the agglomeration of the clay particles as shown in Figure 4.7.

Table 4.4 Surface areas, cumulative pore volumes, and average pore diameters of S80DCII filled with different acid-treated clay content (wt%)

Sample	Surface areas (m^2/g)[a]	Cumulative pore volumes (cm^3/g)[b]	Average pore diameters (nm)[b]
0 wt%	198 ± 9	0.11 ± 0.004	1.51 ± 0.007
1 wt%	237 ± 12	0.13 ± 0.005	1.38 ± 0.007
3 wt%	253 ± 15	0.14 ± 0.007	1.37 ± 0.016
5 wt%	262 ± 10	0.14 ± 0.005	1.36 ± 0.006
10 wt%	523 ± 20	0.21 ± 0.020	1.36 ± 0.003
15 wt%	346 ± 18	0.17 ± 0.005	1.43 ± 0.095

[a] From BET treatment of N_2 adsorption data.

[b] From BJH treatment of N_2 adsorption data.

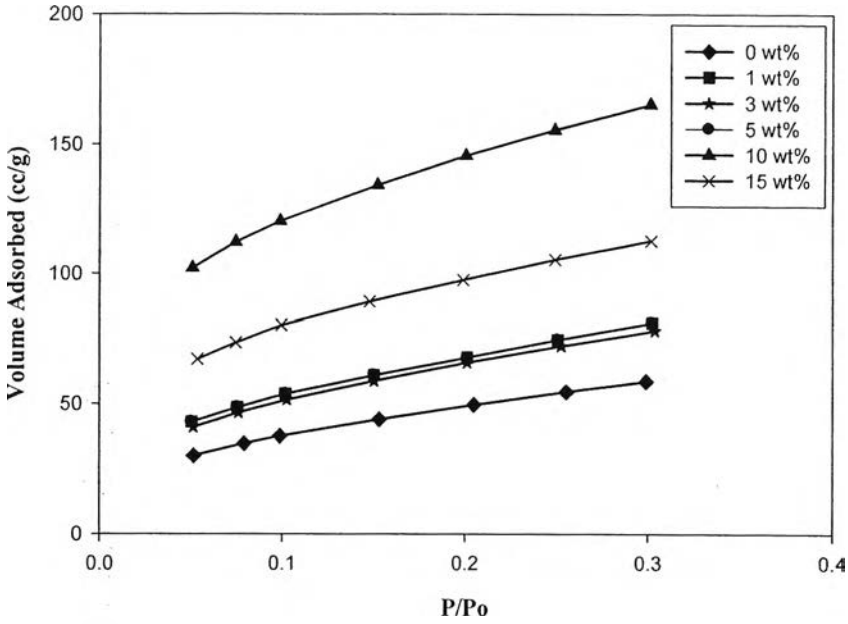

Figure 4.6 Volume adsorbed for S80DCII filled with different acid-treated clay content (wt%).

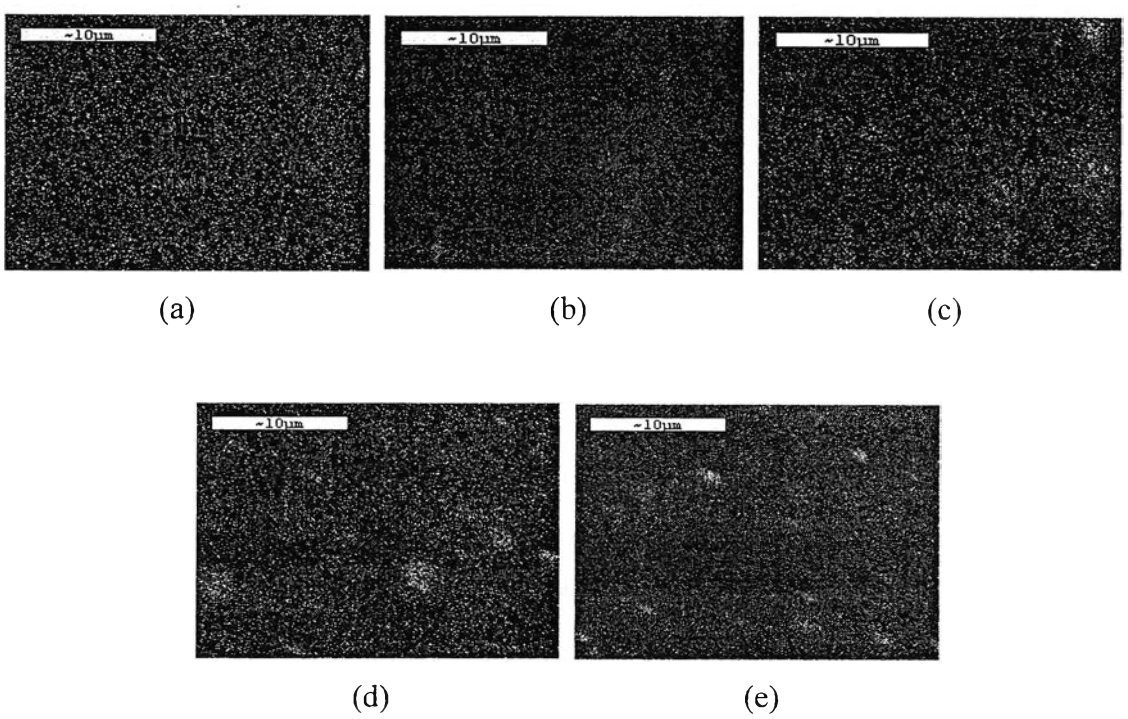

Figure 4.7 SEM-EDX(Si) micrographs of S80DCII filled with different acid-treated clay content (wt%): (a) 1%; (b) 3%; (c) 5%; (d) 10%; (e) 15%.

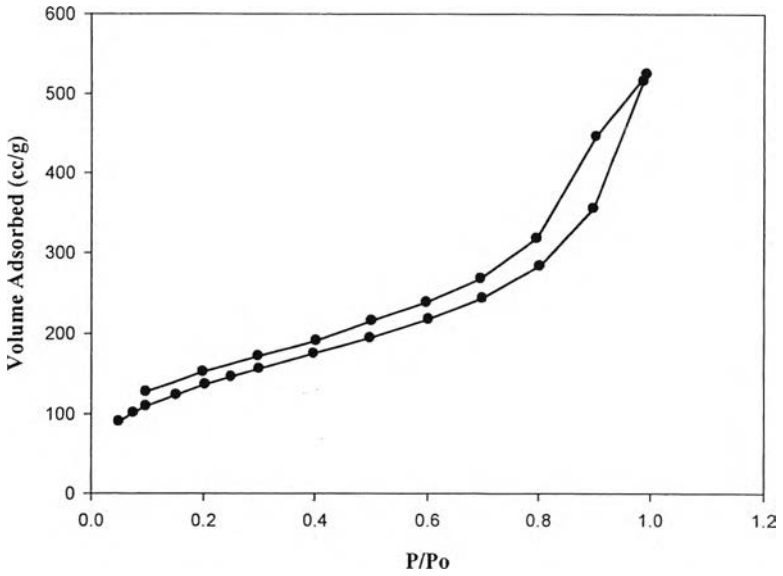

Figure 4.8 Typical example of N_2 sorption isotherm for poly(DVB)HIPE samples in Table 4.3 and Table 4.4.

A typical example of the type of N_2 sorption isotherm for poly(DVB)HIPE nanocomposites is displayed in Figure 4.8, N_2 sorption isotherms of all poly(DVB)HIPE samples listed in Table 4.3 and Table 4.4 are mesoporous materials (type IV). BET isotherm according to the BDDT classification.

4.4.2.2 Thermal properties

TG analysis of poly(DVB)HIPEs, prepared from different mixture of surfactants with different amount of acid-treated clay content, was carried out to measure the thermal stability of the poly(DVB)HIPEs with the temperature range between 40-600°C and heating rate of 10°C/min. TGA thermogram of temperature against percent weight loss are shown in Figure 4.9. It was observed from the thermogram that decomposition behaviors of all poly(DVB)HIPE were in the form of a one step degradation process, and hence decomposition temperature reported the temperature corresponding to 50% decomposition of the material. The thermal decomposition temperature (T_d) and residue yield (%) were listed in the Table 4.5, and the DTG curves of samples as shown in Figure. 4.10.

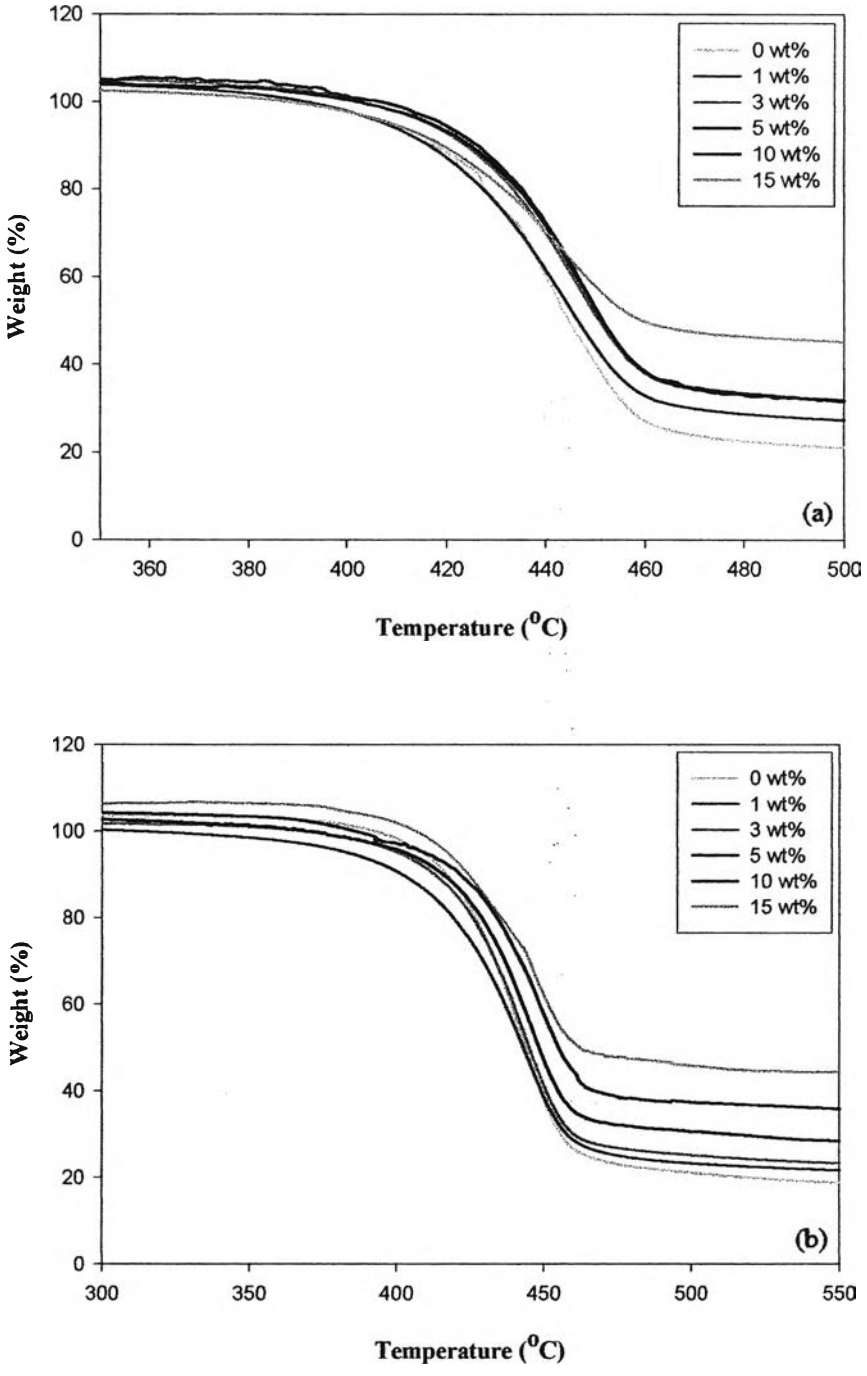

Figure 4.9 TGA thermograms of (a) S80DCI, and (b) S80DCII.

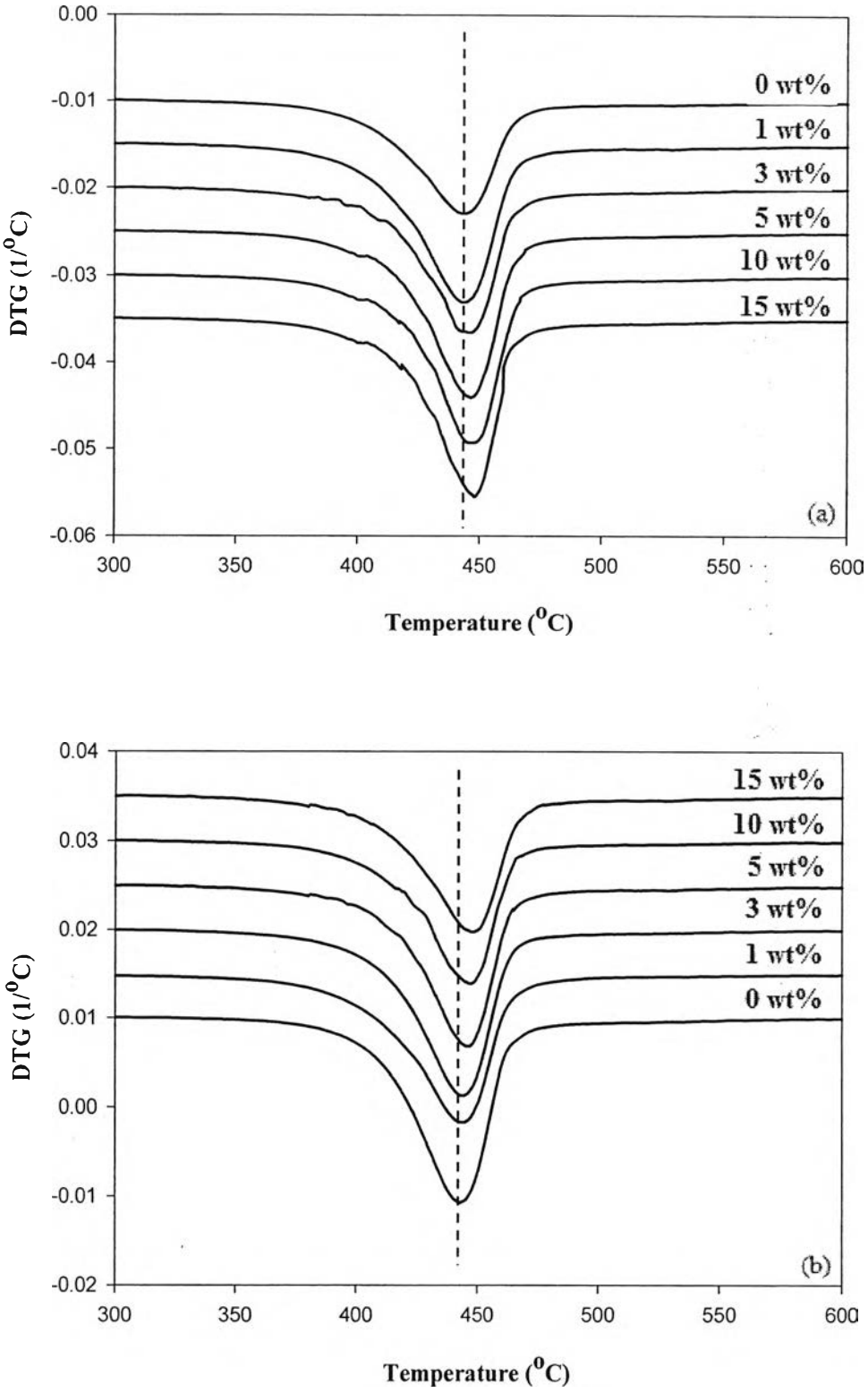

Figure 4.10 DTG curves of (a) S80DCI, and (b) S80DCII.

Table 4.5 Thermal decomposition temperature (T_d) and residue yield (%) of S80DCI and S80DCII filled with different amount of acid-treated clay content (wt%)

Sample	S80DCI		S80DCII	
	T_d (°C)	Residue Yield (%)	T_d (°C)	Residue Yield (%)
0 wt%	444.76	18.0	443.99	18.0
1 wt%	446.47	23.9	443.07	20.9
3 wt%	450.70	28.4	445.13	22.7
5 wt%	451.49	28.4	448.44	29.0
10 wt%	451.36	28.6	454.89	35.2
15 wt%	459.67	42.4	462.03	44.1

It was observed that the decomposition temperature of poly(DVB)HIPE nanocomposites shifted to a high temperature with increasing acid-treated clay content. Residue yield for poly(DVB)HIPE nanocomposites are higher than neat poly(DVB)HIPEs and depended on the acid-treated clay content. This result, indicated that the incorporation of clay nanoparticles into poly(DVB)HIPE offers a stabilizing effect against decomposition: protecting from thermal degradation by keeping the polydivinylbenzene chains and the original molecular structure intact which results in increasing decomposition temperature and residue yield of the obtained polyHIPEs[12].

The glass transition temperature (T_g) of the poly(DVB)HIPEs filled with and without acid-treated clay was investigated by using DSC with the temperature range between 30-250°C and heating rate of 10°C/min. It was found that no glass transition temperature can be detected from both neat poly(DVB)HIPEs and poly(DVB)HIPE nanocomposites (see Figure 4.11). Because, in preparation of poly(DVB)HIPEs, DVB was used as a crosslinking agent as well as a monomer in the organic phase. So, high degree of crosslinking of DVB was obtained leading to absence of a glass transition temperature (T_g). These observations were consistent with the results from many works[13-15], which indicated that no glass transition temperature (T_g) was detected due to the high degree of DVB lead to high degree of crosslinking.

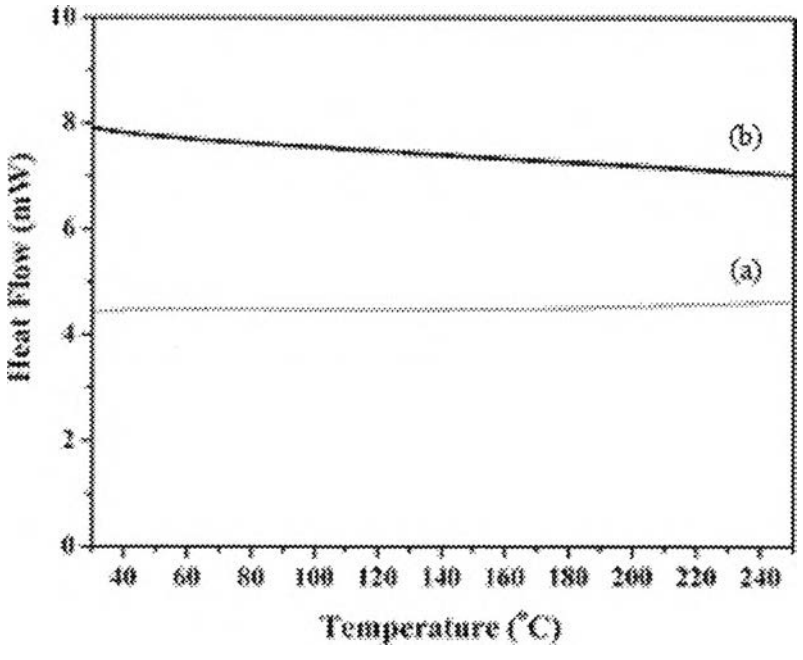

Figure 4.11 DSC thermograms of a) neat poly(DVB)HIPE b) poly(DVB)HIPE nanocomposite.

4.4.2.3 Mechanical properties

4.4.2.3.1 Compressive Response

Mechanical properties of poly(DVB)HIPEs, prepared from different mixture of surfactants with different amount of acid-treated clay content, were carried out. The samples were loaded until a displacement of 70 percent of the height of the examined sample was reached. The compressive stress-extention curve for neat poly(DVB)HIPE and poly(DVB)HIPE nanocomposites as shown in Figure 4.12.

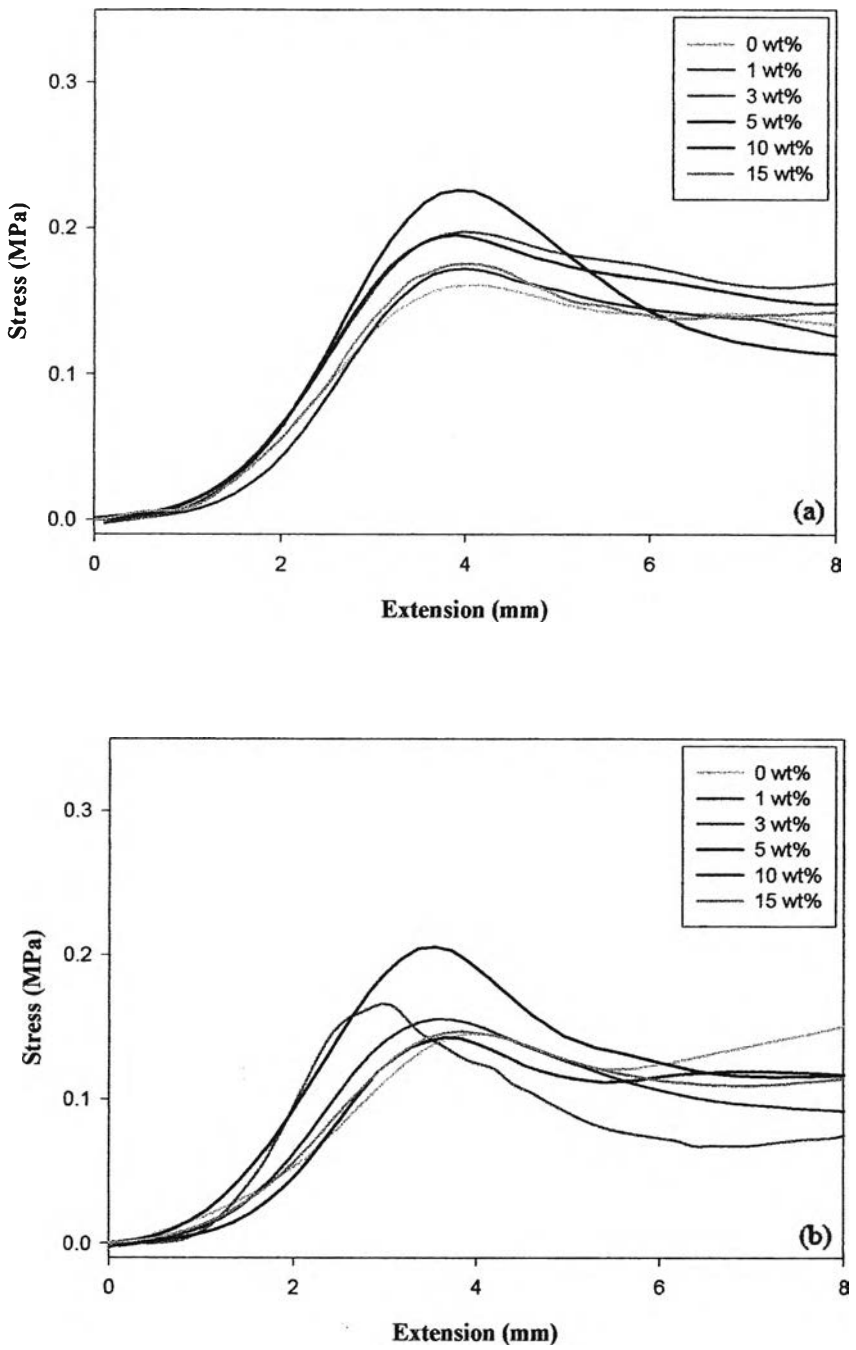

Figure 4.12 Compressive stress–Extension curves of (a) S80DCI, and (b) S80DCII.

The curves show three stages of deformation; initial linear behavior, linear plateau region, and finally, densification. The initial slope is used to calculate compressive modulus of poly(DVB)HIPE and the intersection point between the initial slope and the plateau slope is used to calculate compressive strength. The compressive modulus and compressive strength were listed in the Table 4.6.

Table 4.6 Compressive modulus (MPa) and Compressive strength of S80DCI and S80DCII filled with different amount of acid-treated clay content (wt%)

Sample	S80DCI		S80DCII	
	Compressive Modulus (MPa)	**Compressive Strength (MPa)**	**Compressive Modulus (MPa)**	**Compressive Strength (MPa)**
0 wt%	2.59±0.15	0.13±0.04	2.61±0.27	0.13±0.02
1 wt%	2.87±0.15	0.16±0.03	2.73±0.09	0.17±0.01
3 wt%	2.90±0.14	0.17±0.01	2.90±0.06	0.18±0.01
5 wt%	3.50±0.16	0.24±0.02	3.00±0.10	0.22±0.04
10 wt%	2.80±0.08	0.15±0.01	2.73±0.08	0.16±0.04
15 wt%	2.07±0.10	0.14±0.02	1.99±0.16	0.14±0.04

S80DCI without added acid-treated clay showed compressive modulus and compressive strength of 2.59 and 0.13 MPa, respectively. The compressive modulus and compressive strength of S80DCI filled with 0 to 5 wt% acid-treated clay content, increased from 2.59 to 3.50 and 0.13 to 0.24 MPa, respectively and decreased to 2.07 and 0.14 MPa when acid-treated clay content was 15 wt%. Addition of 5 wt% of acid-trated clay into poly(DVB)HIPE increases its compressive modulus and compressive strength about 35% and 85%, respectively.

S80DCII without added acid-treated clay showed compressive modulus and compressive strength of 2.61 and 0.13 MPa, respectively. The compressive modulus and compressive strength of S80DCII filled with 0 to 5 wt% acid-treated clay content, increased from 2.61 to 3.00 and 0.13 to 0.22 MPa, respectively and decreased to 1.99 and 0.14 MPa when acid-treated clay content was

15 %wt. Addition of 5 wt% of acid-trated clay into poly(DVB)HIPE increases its compressive modulus and compressive strength about 15% and 70%, respectively.

It is observed that both the compressive modulus and compressive strength are higher for poly(DVB)HIPE nanocomposites. Poly(DVB)HIPE nanocomposites exhibited improvement in the mechanical properties of the resulting materials such as compressive modulus and compressive strength when compare to the neat poly(DVB)HIPEs[12]. The maximum improvement was occurred with 5 wt% of acid-treated clay was added to poly(DVB)HIPE matrix. The high aspect ratio and large surface area of acid-treated clay provide the better stress transfer between poly(DVB)HIPE matrix and acid-treated clay, which contributed to the improvement of mechanical performance[16-17]. This situation could be obtained by the addition of acid-treated clay with good dispersion into the continuous phase of poly(DVB)HIPE nanocomposites.

TEM micrographs of poly(DVB)HIPE nanocomposites in Figure 4.13, show that both intercalated and exfoliated dispersed through out poly(DVB)HIPE matrix. However, TEM micrograph with high magnification (×150000), indicated that the well dispersion of acid-treated clay through poly(DVB)HIPE matrix were obtained and resulted in the better stress transfer between two phases. Moreover, At 10 to 15 wt% of acid treated clay content, compressive modulus and compressive strength were decreased because the amount of the added acid-treated clay was high, and resulted in the agglomeration of the clay particles.

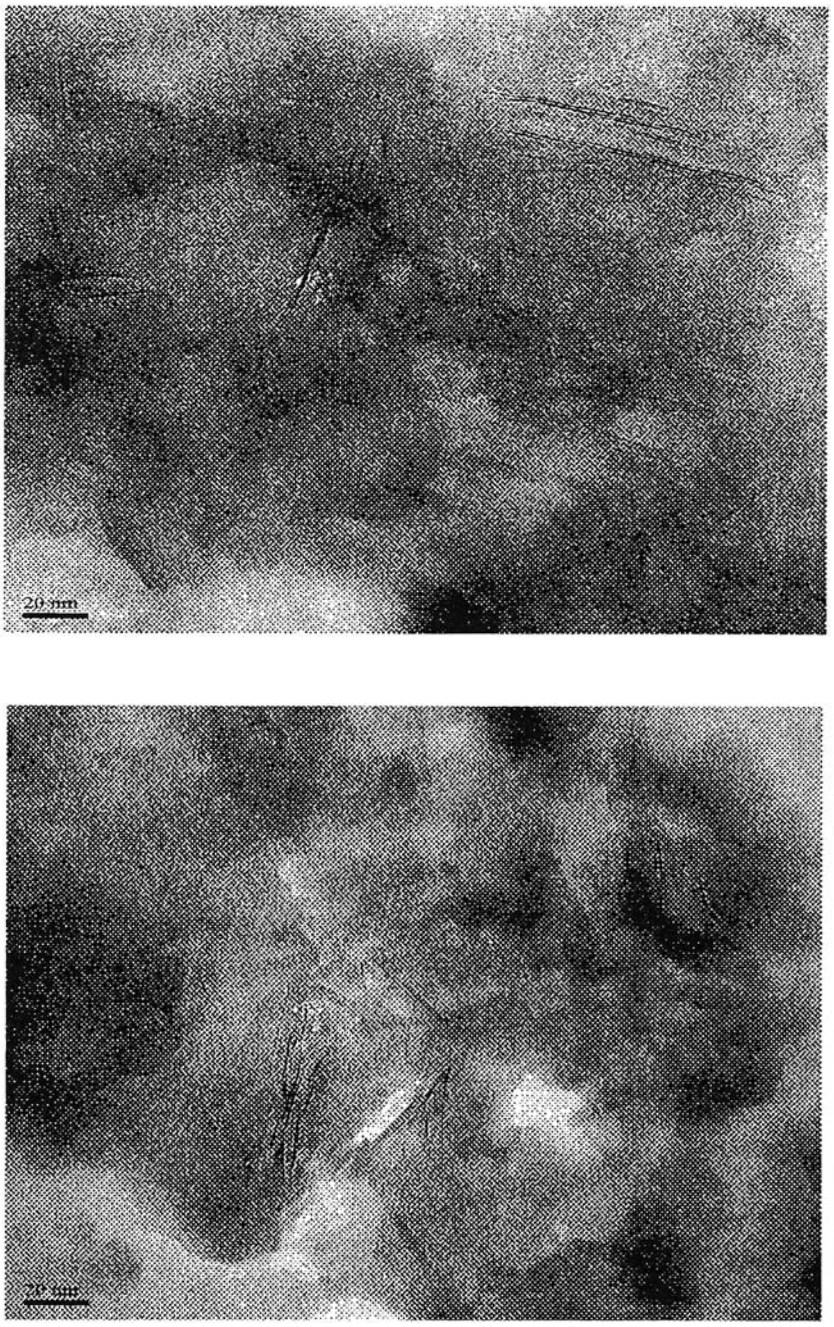

Figure 4.13 High-resolution TEM images of poly(DVB)HIPE nanocomposite.

4.4.2.4 Adsorption capacities

CO_2 gas adsorption of poly(DVB)HIPE, prepared from different mixture of surfactants with different amount of acid-treated clay content, was carried out using a pilot gasification unit at the Department Chemical Technology Department, Faculty of Science, Chulalongkorn university with flow CO_2 3 mL/min

and He 17 mL/min through the sample at room temperature. The CO_2 gas adsorption capacities were listed in Table 4.7.

Table 4.7 CO_2 gas adsorption capacity (mmol/g) of S80DCI and S80DCII filled with different amount of acid-treated clay content (wt%)

Sample	S80DCI	S80DCII
0 wt%	15.9	2.43
1 wt%	18.2	7.97
3 wt%	7.34	6.00
5 wt%	6.45	7.06
10 wt%	2.77	12.3
15 wt%	1.13	8.42

S80DCI without added acid-treated clay showed CO_2 gas adsorption capacity of 15.9 mmol/g. The CO_2 gas adsorption capacity of S80DCI filled with acid-treated clay was found to decreases with increasing content of acid-treated clay added.

S80DCII without added acid-treated clay showed CO_2 gas adsorption capacity of 2.43 mmol/g. The CO_2 gas adsorption capacity of S80DCII filled with acid-treated clay was found to increases with increasing content of acid-treated clay added, and decreases to 8.42 when acid-treated clay content was 15 wt%.

Table 4.8 shows surface area and CO_2 gas adsorption of poly(DVB)HIPEs before and after treated with 3N HCl solutions.

Table 4.8 CO_2 gas adsorption capacity (mmol/g) of S80DCI filled with organo clay and acid-treated clay (wt%)

Sample	S80DCI filled with organo clay		S80DCI filled with acid-treated clay	
	Surface area (m^2/g)	CO_2 gas adsorption capacity (mmol/g)	Surface area (m^2/g)	CO_2 gas adsorption capacity (mmol/g)
0 wt%	549.6	15.9	549.6	15.9
1 wt%	499.4	4.21	501.3	18.2
3 wt%	469.2	4.53	372.4	7.3
5 wt%	447.9	3.92	353.4	6.4
10 wt%	141.3	2.68	346.4	2.8

Poly(DVB)HIPE filled with 1 to 5 wt% of organo clay. The surface area closed to poly(DVB)HIPE filled with acid-treated clay, but CO_2 gas adsorption capacities of poly(DVB)HIPE filled with acid-treated clay showed higher. Therefore, the CO_2 gas adsorption of poly(DVB)HIPE increases after acid treatment. All sample of poly(DVB)HIPEs filled with acid-treated clay exhibited higher adsorption capacity of CO_2 gas when compare with neat poly(DVB)HIPE. Acid treatment of organo clay can improve the gas adsorption of CO_2 due to increasing the surface area, acidity and changes of the chemical composition in the interlayer when compared with poly(DVB)HIPE filled with organo clay.

The correlation of CO_2 gas adsorption capacity by S80DCI and S80DCII with the surface area as shown in Figure 4.14. A large specific surface area was preferable for providing a large adsorption capacity.

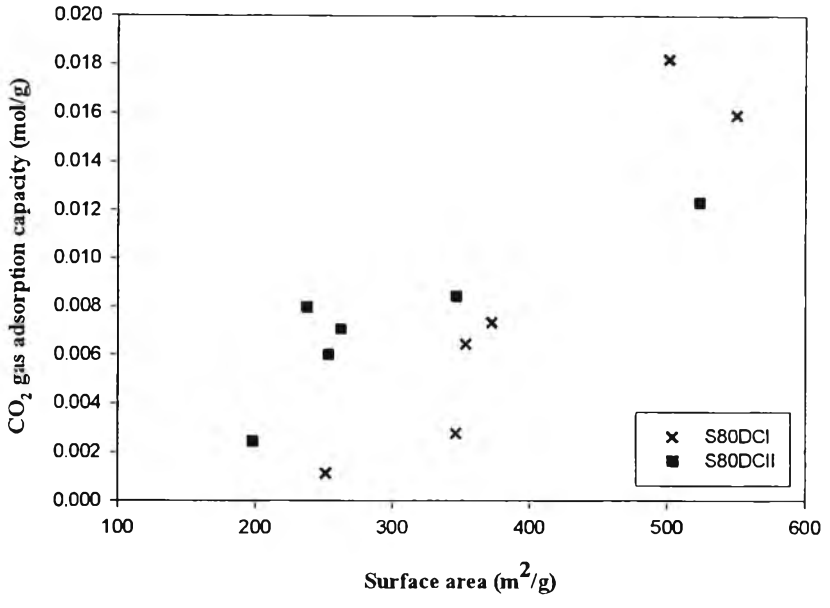

Figure 4.14 CO_2 gas adsorption capacity with the surface area of S80DCI, and S80DCII.

4.5 Conclusions

The clay after acid treatment showed higher specific surface area than before acid treatment. The chemical composition, the structure and the texture of the clay and organo clay after acid treatment influenced the specific surface area of the clay. Clay treated with acid will be incorporated into polyHIPE polymer to increase surface areas, improve mechanical and thermal properties of poly(DVB)HIPE.

Surface areas of S80DCI decreased from 550 to 251 m^2/g. Compressive modulus of the obtained poly(DVB)HIPEs increased from 2.59 to 3.50 MPa with 0 to 5 wt% acid-treated clay content, and decreased to 2.07 MPa when acid-treated clay content was 15 wt%. Decomposition temperature of S80DCI increased from 444.76 to 459.67 °C.

Surface areas of S80DCII with 0 to 10 wt% of added acid-treated clay increased from 198 to 523 m^2/g. Compressive modulus increased from 2.61 to 3.00 MPa with 0 to 5 wt% acid-treated clay content. Surface area and compressive modulus were decreased to 346 m^2/g and 1.99 MPa when amount of added acid-

treated clay content was 15 wt%. Decomposition temperature of S80DCII increased from 443.99 to 462.03 ˚C.

CO_2 adsorption tests were carried out on the obtained poly(DVB)HIPE and it was found that CO_2 adsorption were between 2.4 to 18.2 mmol/g. Highest adsorption was obtained from S80DCI with 1 wt% acid-treated clay.

4.6 References

(1) Barby, D.; Haq, A. *European Patent Application 0 060 138*. **1982**.

(2) Walsch, D.C.; Stenhouse J.I.T.; Kingsbury L.P.; Webster E.J. *J. Aerosol Sci.* **1996**, *27*, 629.

(3) Elmes, A. R.; Hammond, K.; Sherrington, D. C. *European Patent Application 88 303 675.8.* **1988**.

(4) Barbetta, A.; Cameron, N. R. *Materials chemistry* **2000**, *10*, 2466.

(5) Barbetta, A.; Cameron, N. R. *Macromolecules* **2004**, *37(9)*, 3202.

(6) Mills, G.A.; Holmes, J.; Cornelius, E.B. *Journal of Physical and Colloid Chemistry* **1950**, *54*, 1170.

(7) Pakeyangkoon, P., Magaraphan, R., Malakul, P., Nithitanakul, M. *Macromol. Symp.* **2008**. 264, 149.

(8) Venaruzzo, J.L.; Volzone, C.; Rueda, M.L.; Ortiga, J. *Microporous and Mesoporous Materials* **2002**, 56, 73.

(9) Volzone, C. *Applied Clay Science* **2007**, 36, 191–196.

(10) Scamehorn, J.F. *American Chemical Society* **1986,** ACS Symposium Series 311, 1

(11) Dekany, I., Turi, L., Fonseca, A., Nagy, J.B. *Applied clay science* 14 **1999**, 141-160.

(12) Saha, M.C., Kabir, Md.E., Jeelani, S. *Materials Science and Engineering A* **2008**, 479, 213–222

(13) Shim, S. E., Yang, S., Jung, H., Choe, S. *Macromolecular research* **2004**. 12 (2), 233.

(14) Menner, A., Powell, R., Bismarck, A. *Soft matter* **2006**, 2, 337.

(15) Jin, J. M., Lee, J.M., Ha, M. H., Lee, K., Choe, S. *Polymer* **2007**, 48, 3107.

(16) Srinath, G., Gnanamoorthy, R. *J Mater Sci* **2005**, 40, 2897.

(17) Jo, C., Naguib, H. E. *J Cell Plast* **2007**, 43, 111.